GEOPHYSICS, VOL. 75, NO. 6 (NOVEMBER-DECEMBER 2010); P. WB29–WB37, 15 FIGS.
10.1190/1.3481362

Methodology for dense spatial sampling of multicomponent recording of converted waves in shallow marine environments

Nihed Allouche[1], Guy G. Drijkoningen[1], and Joost van der Neut[1]

ABSTRACT

A widespread use of converted waves for shallow marine applications is hampered by spatial aliasing and field efficiency. Their short wavelengths require dense spatial sampling which often needs to be achieved by receivers deployed on the seabed. We adopted a new methodology where the dense spatial sampling is achieved in the common-receiver domain by reducing the shot spacing. This is done by shooting one track multiple times and merging the shot lines in an effective manner in a separate processing step. This processing step is essential because positioning errors introduced during the field measurement can become significant in the combined line, particularly when they exceed the distance between two adjacent shot positions. For this processing step, a particular shot line is used as a reference line and relative variations in source and receiver positions in the other shot lines are corrected for using crosscorrelation. The combined shot line can subsequently be regularized for further processing. The methodology is adopted in a field experiment conducted in the Danube River in Hungary. The aim of the seismic experiment was to acquire properly sampled converted-wave data using a multicomponent receiver array. The dense spatial sampling was achieved by sailing one track 14 times. After correcting for the underwater receiver positions using the direct arrival, the crosscorrelation step was applied to merge the different shot lines. The successfully combined result is regularized into a densely sampled data set free of visible spatial aliasing and suitable for converted-wave processing.

INTRODUCTION

In a shallow marine environment, high-resolution seismic surveys are conducted to solve various geologic and engineering problems (e.g., Pulliam et al., 1996; Marsset et al., 1998; Pinson et al., 2008). Although S-wave information is often necessary to solve these problems, the vast majority of the surveys are designed to acquire P-waves only. This is because S-wave information is generally retrieved from converted waves (Stewart et al., 2003) and these are more difficult to record because they often require deploying the receivers on the seabed. Consequently, the acquisition of this type of wave becomes less efficient and hence more expensive and time-consuming in comparison to the acquisition of P-waves.

Another major obstacle impeding a widespread use of converted waves is the dense spatial sampling required for the data analysis and processing. Depending on the depth of the target and the velocities encountered in the subsurface, the receiver intervals for P-waves are typically 2 to 10 m (e.g., Lucas, 1974; Chapman et al., 2002; Müller et al., 2002) for dominant frequencies between 200 and 650 Hz. The high V_P/V_S ratio in shallow marine sediments imposes a decrease of the spatial interval for S-waves by about the same order. The V_P/V_S ratio near the seafloor varies between 2 in limestones and 13 in water-saturated silts (Hamilton, 1979). Ayres and Theilen (1999) report on V_P/V_S values larger than 30 for unconsolidated sediments found in the Barents Sea. Adequate spatial sampling of S-waves in these sediments requires a receiver interval of less than half a meter.

In marine settings, achieving an adequate spatial sampling is limited in practice by available equipment on the receiver side. Therefore, as in exploration seismology, most effort is made to reduce the shot spacing by minimizing the recording-time length and the boat speed. However, to record the slow converted modes, the recording length needs to be increased. A further decrease of the boat speed is not sufficient to obtain the aimed shot spacing of less than half a meter. Then, seismic surveying for S-wave information becomes not practically feasible.

In this paper, we present a novel methodology developed to achieve properly sampled multicomponent data suitable for converted-wave analysis and processing. In this method, we propose to obtain the required sampling interval on the source side. This is done by shooting the same track multiple times and combining the shot lines together. Inherent to this acquisition approach, the source and re-

Manuscript received by the Editor 3 March 2010; revised manuscript received 22 May 2010; published online 22 December 2010.
[1]Delft University of Technology, Department of Geotechnology, Delft, The Netherlands. E-mail: n.elallouche@tudelft.nl; g.g.drijkoningen@tudelft.nl; j.r.vanderneut@tudelft.nl.

ceiver positioning has to be very accurate for a successful combination of the shot lines to a densely sampled one. Because the positioning errors involved in a typical survey are generally larger than the aimed sampling interval of few tens of centimeters, we introduce an additional processing step to merge the lines together. For this purpose, we use a method based on crosscorrelation to correct for the positioning errors of the shot lines with respect to one reference shot line. The effectiveness and the sensitivity of the crosscorrelation step will first be demonstrated using a synthetic data example before being applied to field data.

As in the case of P-wave surveys, the spacing in the combined shot line is variable and needs to be regularized to ensure adequate handling by processing algorithms. Many techniques related to particular transforms, such as the Fourier transform and the parabolic Radon transform (e.g., Kabir and Verschuur, 1995; Duijndam et al., 1999), were developed over the last decades to reconstruct missing traces. One of these techniques can be applied to the combined shot line to obtain dense and regular sampled data along the spatial direction. In the field example provided in this article, we use the Fourier transform to regularize the data.

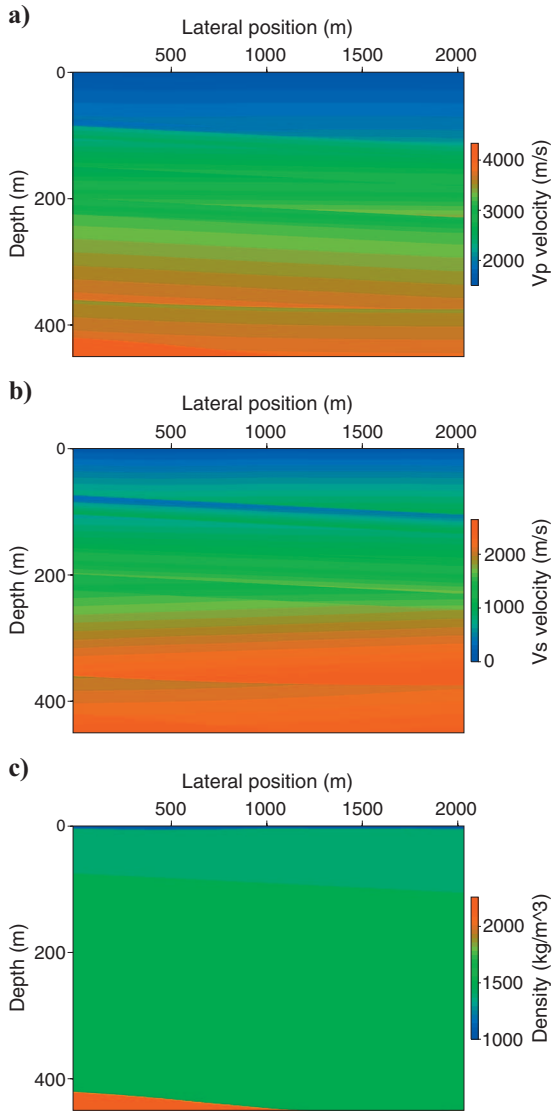

Figure 1. Model used to compute synthetic data: (a) P-wave velocities, (b) S-wave velocities, and (c) densities.

METHODOLOGY FOR DENSE SPATIAL SAMPLING

Shooting multiple lines for the same track

To avoid spatial aliasing, the smallest apparent wavelength of interest in the horizontal direction $\lambda_{\min}$ needs to be sampled at least twice. In turn, the smallest wavelength is determined by the maximum source frequency of interest $f_{\max}$ and the smallest apparent velocity in the subsurface $V_{\min}$ as indicated in this relation:

$$\Delta x \leqq \frac{\lambda_{\min}}{2} = \frac{V_{\min}}{2f_{\max}}. \quad (1)$$

Typically, in high-resolution seismics, sources with a frequency content above 100 Hz are used. In general for P-waves, the smallest velocity encountered in a marine environment is the velocity of sound in water. To record P-waves with a maximum frequency of 250 Hz, and thus a minimum apparent wavelength of 6 m, the data have to be acquired with a spatial interval of at most 3 m. However, for an adequate spatial sampling of S-waves in unconsolidated sediments with a V_P/V_S ratio of at least 10, the spatial sampling needs to be in the order of 0.3 m. This value is very small and not feasible with the standard recording equipment for marine settings.

Consequently, the aimed spatial sampling has to be achieved in a different manner. Because the shots in marine acquisition can be fired much faster and are cheaper compared to land seismics, repeating a shot line multiple times is a logical step to obtain better spatial coverage.

Combining multiple shot lines using crosscorrelation

The simple idea of acquiring multiple shot lines and combining them based on their relative positions is complicated by the measurement errors introduced during the survey. These errors are caused by uncertainties in the positioning system and variation of field conditions over time. After combining the shot lines, these errors may even exceed the distance between two adjacent shot points and result in discontinuities of events and degradation in the resolution of the data. This type of problem is often encountered in high-resolution seismics and is solved by inverting for more accurate source and receiver positions (He et al., 2009). An inversion-based approach is not preferred in our case because the shot redundancy of the data requires repeating the computationally intensive inversion for each shot position. Alternatively, we can correct for the errors using a crosscorrelation-based method.

Crosscorrelation-type techniques have been used to estimate static shifts (Taner et al., 1974), to quantify time-lapse effects (Hale, 2009), and to redatum wavefields (Schuster and Zhou, 2006). Here, we use crosscorrelation to fit the different shot lines within one reference shot line. Each trace from the remaining shot lines is crosscorrelated with a panel of traces from the reference line to estimate its new relative position. The basic idea and the sensitivity of the method are discussed below using a synthetic data example.

Synthetic data example

To explain the idea, we use a synthetic data set computed using a finite-difference algorithm for the model depicted in Figure 1. The

velocities in this model are typical for a shallow sea subsurface composed of soft sediment overlying dipping consolidated rocks. The water bottom is modeled as a rough interface at 20-m depth from the free surface. We computed the pressure for one receiver located on the water bottom and multiple sources located in the water; the shot spacing is 3.5 m. We generated another data set with shot positions shifted half the shot spacing and assigned erroneous random offset values to it. The crosscorrelation procedure is used to correct the offsets and merge these two data sets.

The procedure is explained in Figure 2 for one trace. The erroneous offset value of this trace (x_{er}) is used initially to select a panel of traces from the reference data set which includes all the traces with offset values between $x_{er} - e_{max}$ and $x_{er} + e_{max}$; e_{max} is the largest spatial error expected in the measurement. Subsequently, the erroneous trace is crosscorrelated with the panel and the result is shown on the right part of Figure 2a. The traces that have their maximum amplitude at the smallest positive and negative time lags are basically located adjacent to the erroneous trace. The new offset value of the erroneous trace x_{tr} can then be linearly interpolated from the values of its neighboring traces:

$$x_{\mathrm{tr}} = x_1 + \frac{\Delta t_1}{\Delta t_1 + \Delta t_2}(x_2 - x_1), \qquad (2)$$

where x_1 and x_2 are the offset values of the adjacent traces and Δt_1 and Δt_2 are their corresponding time lags from the output correlation panels. The newly computed offset value x_{tr} is then used to merge the trace into the panel. As shown in Figure 2b, this procedure is very effective because the trace is placed at the right position. We implemented the idea further by repeating the procedure for the remaining traces. When the crosscorrelation fails to correct for the offset, the trace is not merged in the reference line. The successfully combined result is compared to the reference data set in Figure 3. It can be noticed that the combined data set is interpolated because it is composed of twice the number of shots compared to the reference data. The small differences between the two data sets, indicated by the black arrows, are the result of excluding the traces that were corrected by a value exceeding e_{max}.

Sensitivity of the method

The aim of the crosscorrelation step is to reduce the relative uncertainties in offsets introduced during the field acquisition by different factors. These errors are difficult to quantify and can vary from one shot position to another. The linear interpolation of offsets is correct for linear events like the direct wave, refracted waves, and interface waves, and is an approximation for hyperbolic-shaped reflections. This approximation may break down when the initial gap between the adjacent sources in the reference line is too large.

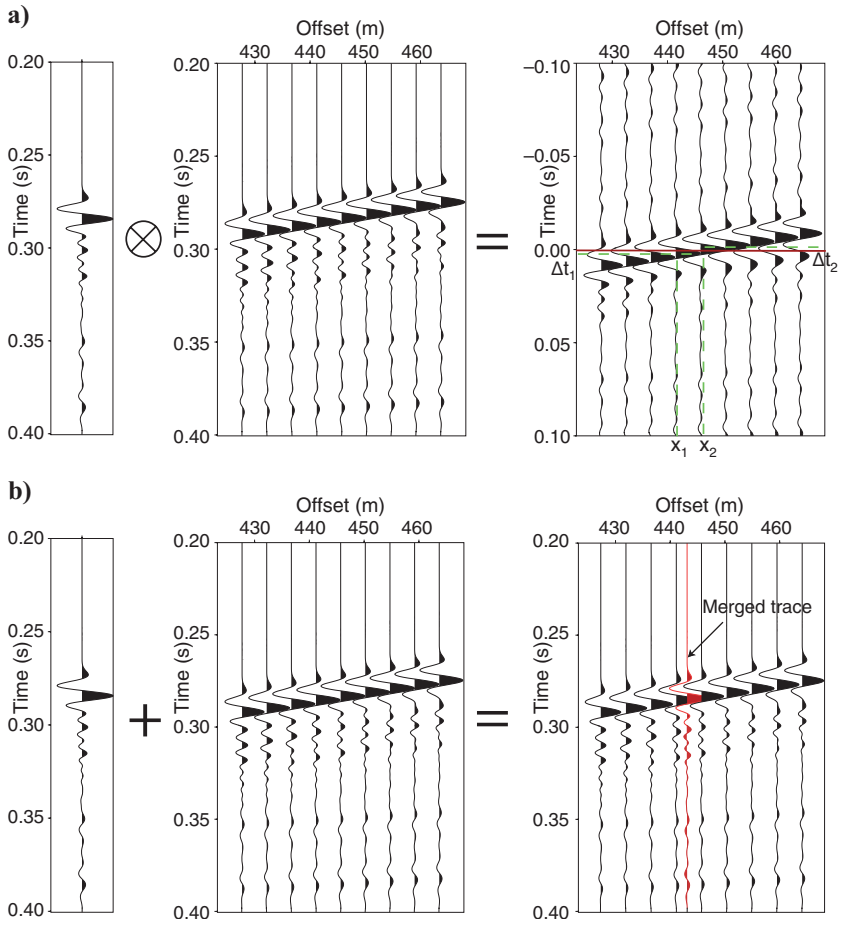

Figure 2. Illustration of the offset-correction procedure for one trace using crosscorrelation. (a) An arbitrary trace with an erroneous offset is crosscorrelated with a panel of traces from the reference line. (b) The trace with the newly computed offset value (in red) is merged into the panel.

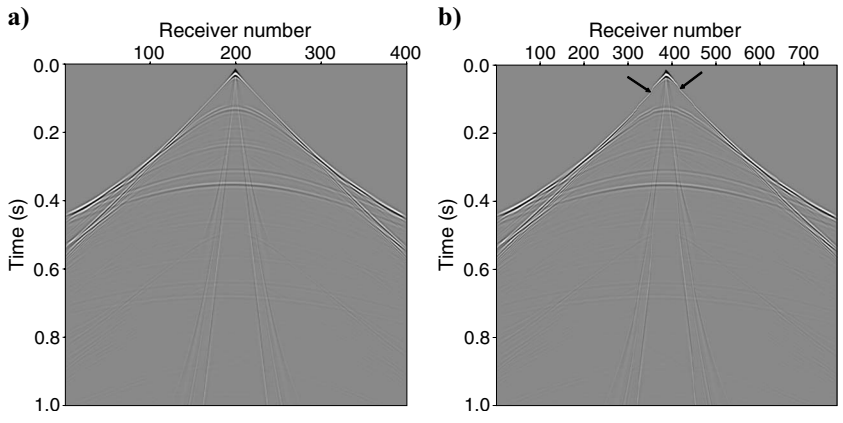

Figure 3. (a) The reference common-receiver gather and (b) the common-receiver gather combined using crosscorrelation. Black arrows indicate differences corresponding to locations of traces which were not merged by crosscorrelation.

To test the sensitivity of the method to the initial source spacing, we generated four data sets with their corresponding reference common-receiver gathers. The source spacings of the reference data sets are 3, 4.5, 6, and 9 m. The offset values of the data are set to different values, by assigning random values to the traces with a maximum deviation of 4 m. The data sets are subsequently crosscorrelated with their corresponding reference shot gather and the offset values are corrected. The absolute errors in offset between the data set before and after the correction step for each source spacing are shown in Figure 4.

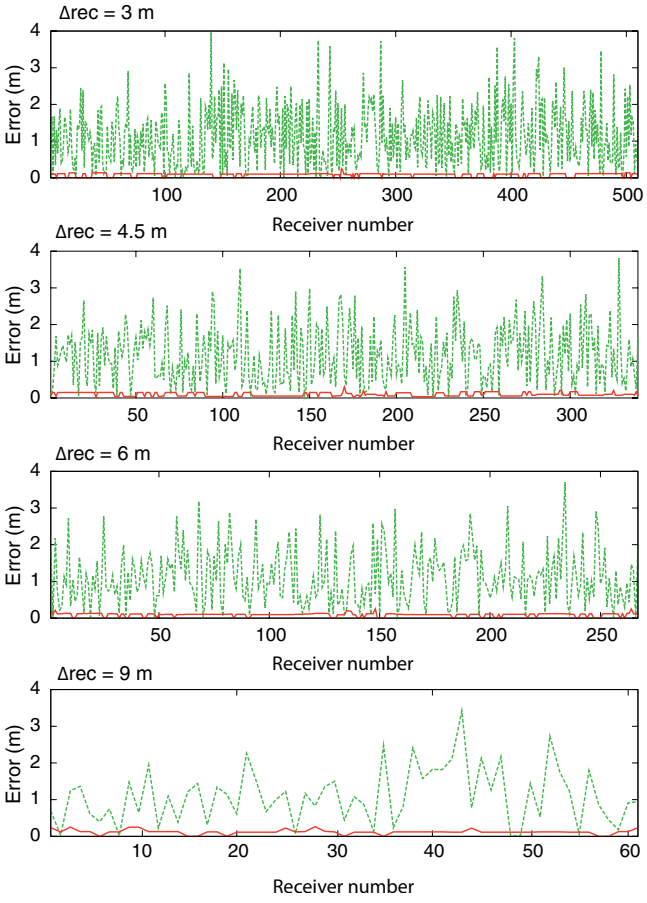

Figure 4. Absolute errors in offset before (green dashed lines) and after (red solid lines) applying the correction step using crosscorrelation. Errors are computed for source spacing of 3, 4.5, 6, and 9 m.

The green lines in Figure 4 indicate the initial errors which are comparable to the positioning errors introduced during the measurement, whereas the solid red lines are the final errors after applying the crosscorrelation step. It can be noticed that the correction method using crosscorrelation effectively minimized the absolute errors independently from their initial values. Moreover, the method proved to be insensitive to the shot spacing of the reference line. This implies that the effectiveness of the crosscorrelation is mainly determined by the strong linear direct or refracted events.

Another factor which may affect the result of the crosscorrelation step is noise. Real data can be very noisy, particularly at far offsets, and the noise may have the same bandwidth as the data. We added incoherent Gaussian-distributed noise in the frequency range of 20–250 Hz to the generated reference data shown in Figure 3a and applied the crosscorrelation step again. Because of the presence of noise in the data, the number of the successfully merged traces is drastically reduced as can be noticed when Figure 5a is compared to the noise-free data in Figure 3b. For many traces, the maximum crosscorrelation amplitude was affected by noise, resulting in a wrong offset interpolation. Omitting these traces from the merged data set resulted in an irregular source spacing and a ragged appearance of arrivals. In this condition, time-gating the direct arrival and applying a bandpass filter before the crosscorrelation procedure help increase the number of successfully merged traces as shown in Figure 5b.

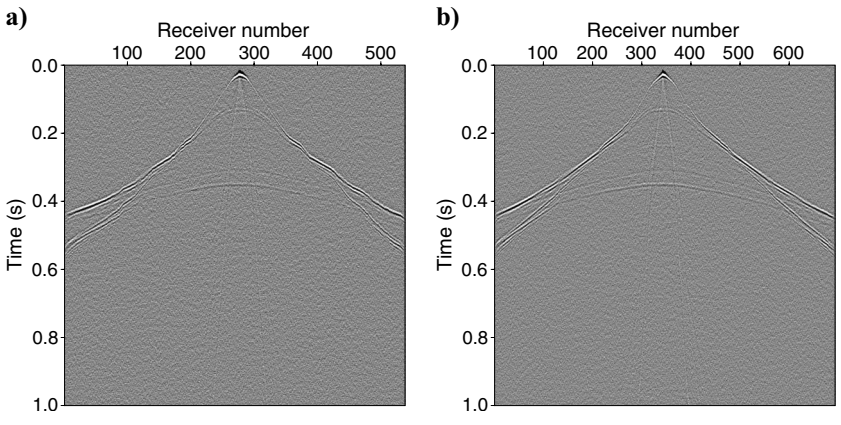

Figure 5. Combined data sets after addition of Gaussian-distributed noise in the frequency range from 20 to 250 Hz. (a) Only crosscorrelation is applied and (b) crosscorrelation is preceded by time-gating the direct arrival and bandpass filtering (30–120 Hz).

FIELD EXPERIMENT IN THE DANUBE RIVER

Data acquisition

A high-resolution seismic survey was conducted on the Danube River in 2008 near the village of Kulcs, Hungary. The aim of the survey was to acquire properly sampled seismic data suitable for converted-wave processing. For this purpose, we adopted the methodology proposed above.

The survey area is located in a seismically active region south of Budapest. The shallow subsurface is composed of Miocene unconsolidated sand and shale sequences underlying young river sediments. Figure 6 shows the study area and the approximately 1-km-long seismic track shot using an air gun.

The data were recorded using a 4C water-bottom cable consisting of 12 receivers with a spacing of 5 m. The cable was deployed on the riverbed at a depth of 3.5 m. A 20-in^3 air gun was towed at a depth of 2 m and fired every 4 s. The data were digitized at a time-sampling interval of 0.250 ms with a recording length of 2 s. By firing the air gun only in the upstream direction, the boat speed was minimized to ~1 m/s, resulting in a shot spacing of ~4 m. Given the frequency content of the source and the S-wave velocities expected in river sediments, we aimed at a spatial sampling interval of 0.3 m. To achieve this, we shot 14 times along the same track.

During the survey, positioning errors were introduced by different causes: (1) the positions of the receivers on the river bottom are not exactly known, (2) possible variation of the receiver positions with time because of the strong currents in the water, (3) the GPS system was towed 3 m behind the source for protection (also, because of the currents in the water, it was difficult to align them), and (4) the inaccuracy of the used positioning systems. These errors impede a combination of the shot lines without deteriorating the lateral resolution of the data.

In the methodology discussed above, the crosscorrelation step is applied to account for the variation of positioning errors between the shot lines by correcting their offset values with respect to one reference shot line. The offset values of the reference shot line are assumed to be correct because they are used for the offset interpolation. However, to be able to apply the crosscorrelation step to the field data, the positioning errors introduced during the field survey need to be corrected for a single shot line that we will use as a reference line.

While the error related to the source position is easily corrected, the uncertainty involved with the underwater receiver positions required a separate procedure to minimize it. In the processing flow, we first estimate the receiver positions using the direct arrival, before we use crosscorrelation to merge the shot lines together. The combined result will then be regularized using the nonuniform discrete Fourier transform and filtered to remove the low frequency interface waves strongly present in the data. All the processing steps are applied in the common-receiver gather domain.

Estimation of receiver positions using direct arrival

In the field, the first and last positions of the receiver array were measured before its release into the water. However, from the near-offset traces, the uncertainties in receiver positions appeared to be unacceptably large and required correction before further processing could be applied. Assuming that the shot positions are correct, we make use of the direct wave recorded as the first arrival in the nearest offsets to estimate the correct coordinates of each receiver. We account for the depth difference between source and receiver measured in the field and we apply normal-moveout (NMO) correction to the near-offset traces using the water velocity of 1500 m/s×. The alignment of the direct wave in each common-receiver gather after NMO is an indication of the accuracy of the coordinate. The NMO-corrected traces are stacked and the first arrival is time-gated to determine the mean stacking amplitude. The procedure is depicted in Figure 7.

This procedure is repeated for receiver coordinates varied over a grid of 20 × 20 m around the measured position. The mean stacking amplitude computed for each grid point is mapped in Figure 8. The elliptic red area corresponds to the coordinates with the highest stacking amplitude. The new receiver position is determined by picking the grid point with the maximum amplitude. The elongated shape of the red area indicates that the position is not well-constrained in the direction perpendicular to the shot lines. Figure 9 shows the measured and estimated receiver positions with respect to the shot lines.

The receiver position is estimated separately for all the shot lines where the positioning-related errors (trigger delays, navigation problems, instrumentation defects, etc.) other than the ones discussed above are discarded. The shot line that provided the best constrained receiver coordinates is selected as a reference shot line.

Merging shot lines using crosscorrelation

The necessity of the crosscorrelation step is demonstrated in Figure 10. The combination of only three shot lines according to their offset resulted in jittering and discontinuities in the recorded events and in the degradation of the lateral resolution. Although we reduced the errors related to the source and receiver positions before computing the offset, it is clear that this is not sufficient because of the variations of these errors between the shot lines.

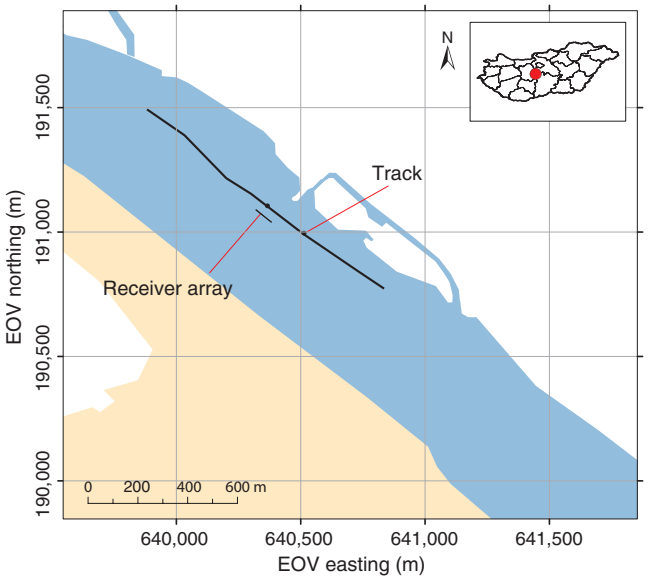

Figure 6. Map of the survey area showing the track of the shot lines in Hungarian state plane-coordinates (EOV).

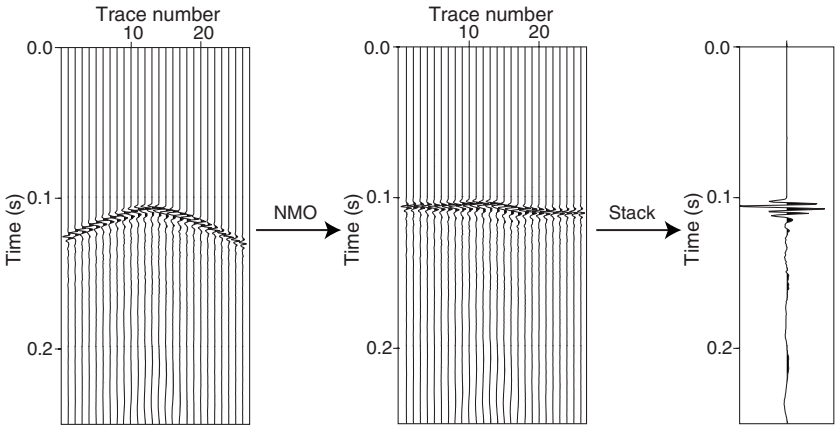

Figure 7. Procedure of estimating the receiver positions: common-receiver gather containing near-offset traces only (left), normal-moveout correction applied (middle), and the stacked trace (right). The first arrival of the stacked trace is time gated and the mean amplitude is determined.

The shot lines are merged by crosscorrelating each of their traces with a panel of traces from the reference line selected according to their offsets within 20 m range from the erroneous offset of the trace. In the crosscorrelated panel, the minimum positive and negative time lags and the offsets of their corresponding traces are picked and used as given in equation 2 to estimate the new offset value of the trace. The data are also interpolated in time (by a factor of 5) in order to pick time lags more accurately.

Difficulties arise at noisy traces and far offsets where the signal-to-noise ratio is relatively low. Consequently, picking the right maximum amplitude becomes hard and traces can end up at the wrong position. Bandpass filtering is applied to minimize the low-frequency noise that was mainly present in the two horizontal components Vx and Vy. Given the fact that the 3C geophones were located at the same position in the field, the crosscorrelation results of the three receiver gathers are compared and combined to increase the number of successfully merged traces. This approach was particularly beneficial for the Vy component because many of the traces were initially not properly corrected because of the relatively weak signal recorded in this direction. The procedure, finally, combined almost 4000 traces (slightly more for the pressure component), covering a distance of 1 km to one spatially dense common-receiver gather as shown for the four components in Figure 11.

Although the effects caused by the crossline offset in the data were not accounted for, it can be observed that the continuity of all the events is well preserved in the four components after the merging procedure. This implies that these effects are negligible in this case. However, in general, strong lateral variation in the crossline direction is expected to degrade the resolution of the data.

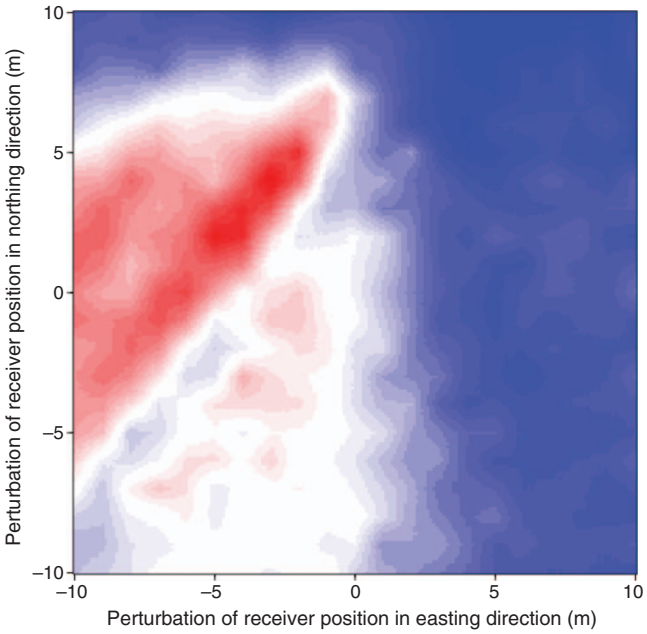

Figure 8. Mean stacking amplitude mapped on the receiver-perturbation grid.

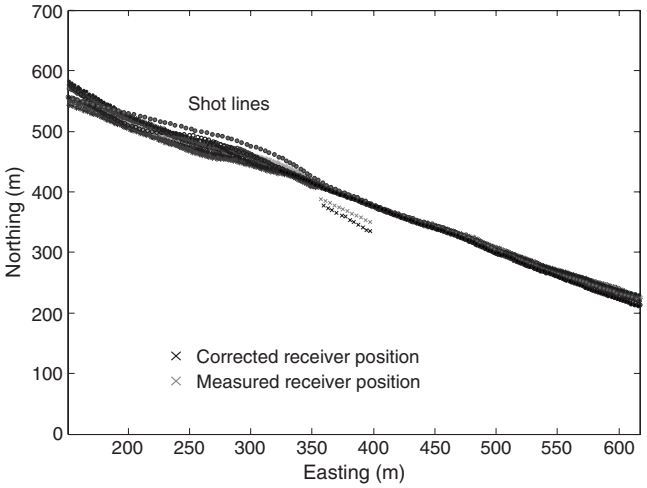

Figure 9. Map showing measured and corrected receiver positions with respect to the 14 sailed shot lines.

Regularization

The crosscorrelation step resulted in densely sampled receiver gathers with shot spacing varying between 0.1 and 3 m. Because most processing algorithms require a constant spatial interval, the obtained data are regularized. Various regularization techniques exist but we used the nonuniform discrete Fourier transform and the discrete inverse Fourier transform to achieve a regular shot spacing. The data in the spatial Fourier domain is obtained using the Riemann sum (Duijndam et al., 1999):

$$\tilde{P}(k_x,\omega) = \sum_{n=0}^{N-1} P(x_n,\omega) e^{jk_x x_n} \Delta x_n, \tag{3}$$

with a variable spatial interval Δx_n defined as

$$\Delta x_n = \frac{x_{n+1} - x_{n-1}}{2}, \tag{4}$$

where x_n is the sample location, k_x is the wavenumber, and ω is the temporal frequency.

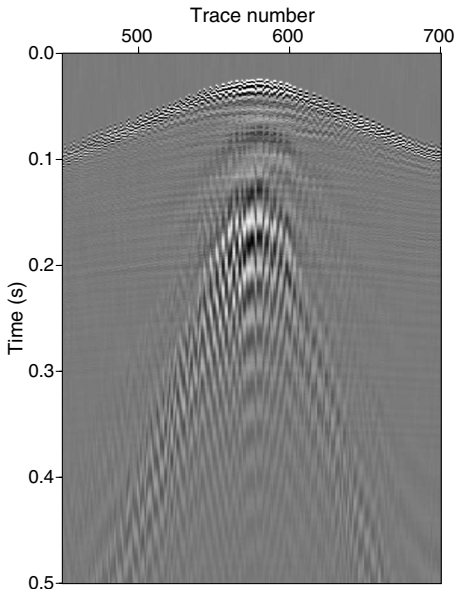

Figure 10. Part of a common-receiver gather of the pressure recording showing jittering and discontinuities resulting from combining three shot lines.

Figure 12 shows the *f-k* spectra of common-receiver gathers recorded with the hydrophone and the horizontal component of the geophone. The amplitude spectrum obtained from transforming a common-receiver gather from one shot line with an average spacing of 4 m is compared to that of the combined line. The spatial aliasing of reflections and interface waves so obviously visible in Figure 12a

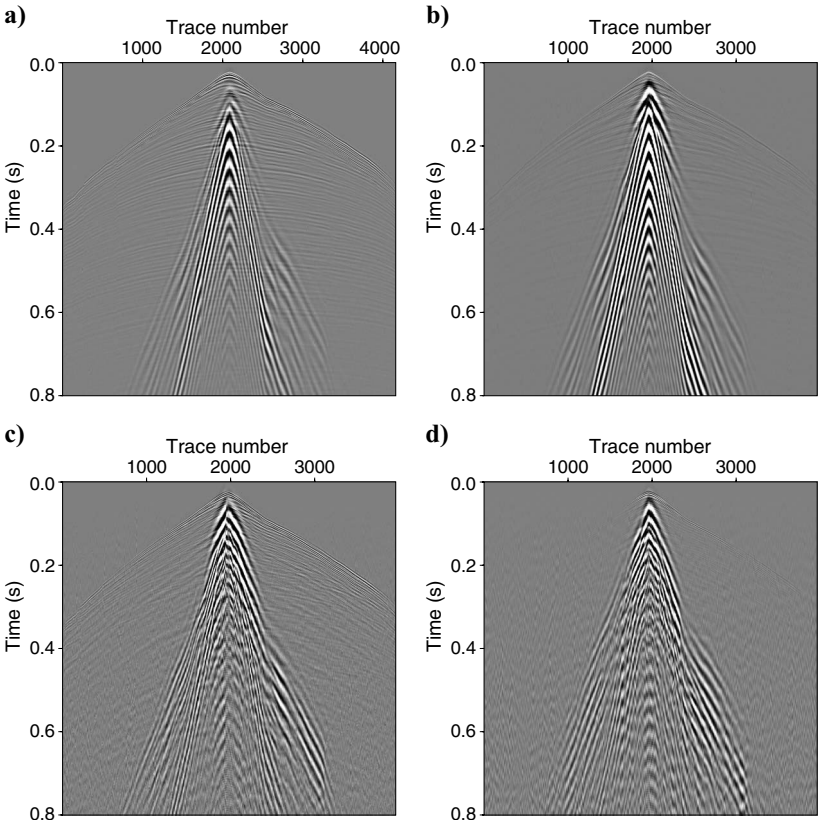

Figure 11. The combined common-receiver gathers after applying the crosscorrelation step. (a) Pressure, (b) vertical (Vz), (c) horizontal inline component (Vx), and (d) horizontal crossline component (Vy).

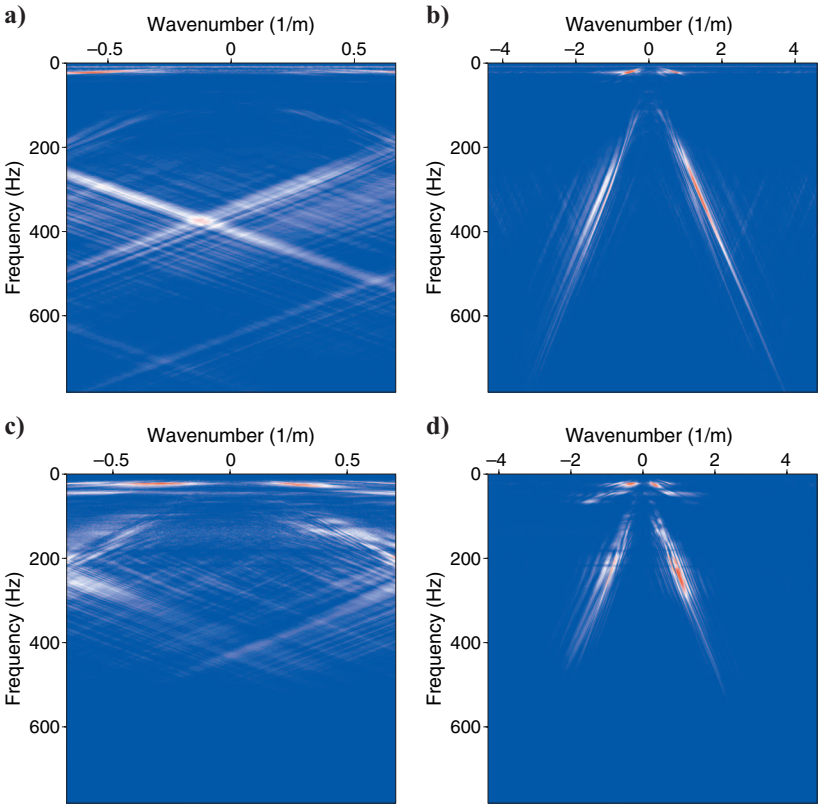

Figure 12. Comparison of the *f-k* spectrum of the reference line with that of the combined line. (a) Reference line of recorded pressure, (b) combined line of recorded pressure, (c) reference line recorded by the horizontal component, and (d) combined line recorded by the horizontal component.

and c is no longer present after combining all the shot lines (Figure 12b and d).

The regularized data are then obtained by transforming the data back to the time domain using the uniform inverse Fourier transform in the spatial direction, given by

$$P(x,\omega) = \frac{\Delta k_x}{2\pi} \sum_{m=-M}^{M} \tilde{P}(m\Delta k_x,\omega) e^{-jm\Delta k_x x}; \qquad (5)$$

Δk_x has to be small enough to avoid aliasing. We have chosen a value equal to half the maximum offset in the data. For Δx, we selected a constant spatial interval of 0.5 m, which is larger than the aimed interval of 0.3 m, but it was found adequate for the acquired data. The low frequency interface waves, dominant in all components, are removed from the data using an f-k filter before transforming the data back to the time domain. Figure 13 shows the four regularized components for one common-receiver gather. As expected, the P-wave reflections are mainly present in the pressure and vertical components, whereas the converted modes can be identified in the horizontal inline component. Part of the data, enclosed in the black frames in Figure 13, is enlarged in Figure 14, where the converted modes are compared to the P-wave reflections. Low apparent velocity and horizontal polarization are distinctive features of PS-waves.

The steps of the proposed methodology are summarized in Figure 15 for a small number of traces from the vertical component data. It can be noticed that we indeed succeeded to achieve a dense and regular spatial sampling without deteriorating the continuity of both the high-frequency first arrivals and the low-frequency interface waves.

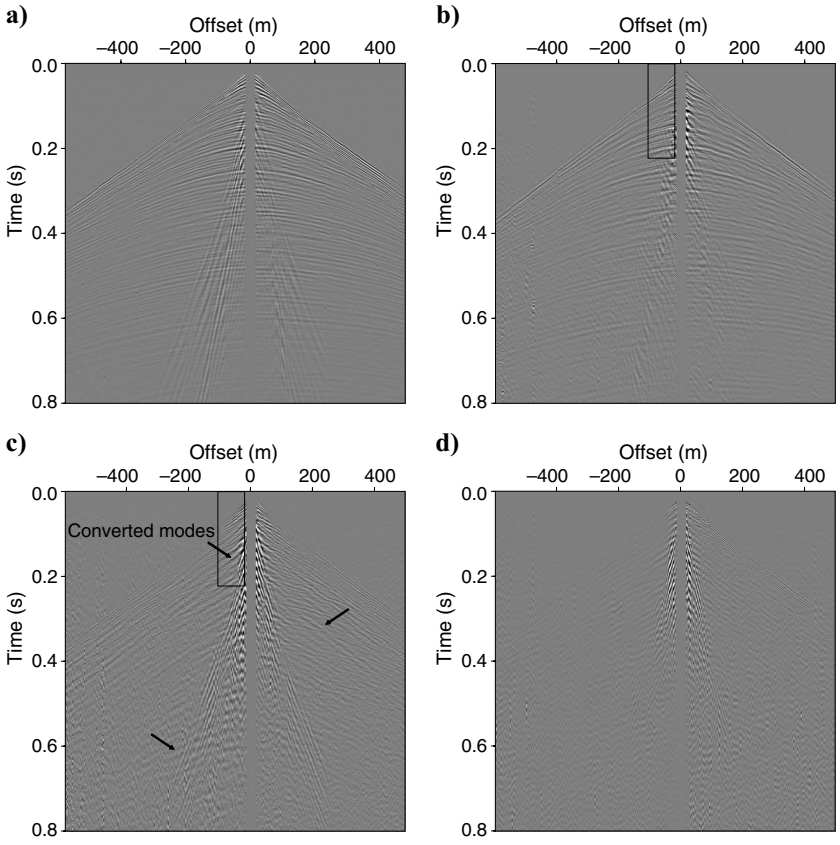

Figure 13. Combined shot lines after regularization: (a) pressure, (b) vertical component, (c) horizontal inline component (Vx), and (d) horizontal crossline component (Vy). The black arrows indicate different converted modes identified in the horizontal inline component. The data captured in the black frame are enlarged in Figure 14.

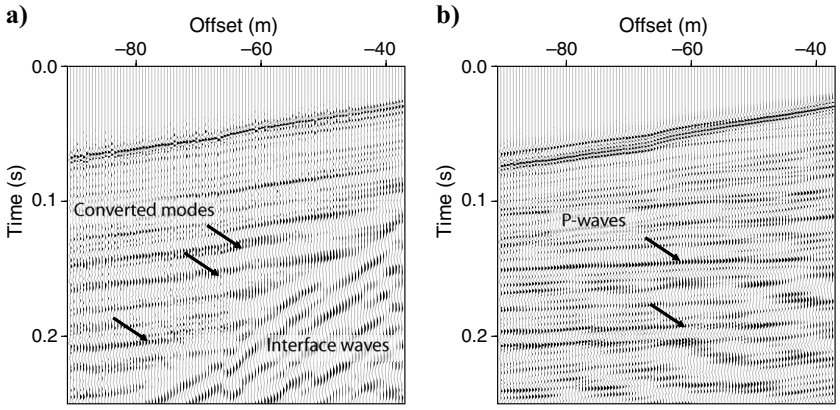

Figure 14. Enlarged part of the horizontal inline component is compared to the vertical component. Black arrows indicate different converted modes in the horizontal component and two prominent P-wave reflections in the vertical component.

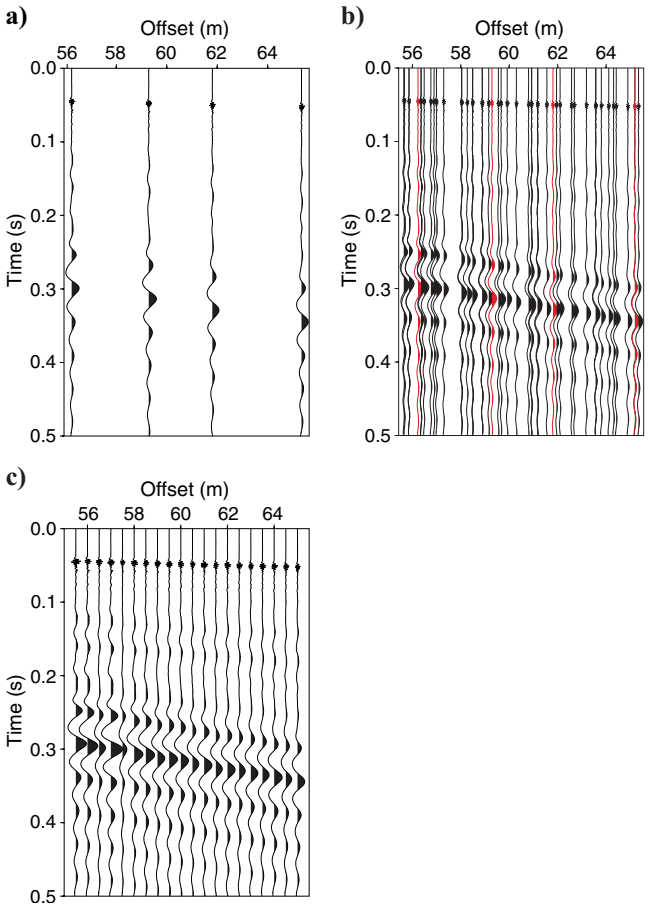

Figure 15. The different steps of the methodology illustrated using a small number of traces from the vertical component: (a) reference shot line, (b) combined shot line (red traces are from the reference shot line), and (c) combined shot line after regularization.

CONCLUSIONS

We developed a novel methodology aimed at acquiring seismic data recorded on the seabed and suitable for converted-wave processing. To avoid spatial aliasing, the primary focus of the method is on achieving spatially dense data by sampling one track multiple times. The shot spacing is then reduced by combining the shot lines together. Inevitably with this method, the navigation of the sailed lines must be very precise and variation in source and receiver positions must be minimized.

The crosscorrelation step proved to be very effective in reducing the relative error in positioning between a reference shot line and the remaining lines. In the synthetic data example, we showed that the processing step is insensitive to the gap between the shots in the reference line and the magnitude of the error involved, when the direct arrival is strongly present. The method is, however, affected by noise.

The devised methodology was successfully employed in a field experiment conducted in the Danube River, in Hungary. The source and receiver-position errors of one specific shot line were quantified and corrected for. A special procedure was applied to estimate the underwater receiver positions using the direct arrival. This procedure reduced the error in the direction parallel to the shot lines but the error was not well-constrained for the direction perpendicular to them. Time interpolation and bandpass filtering were needed to enhance the results of the crosscorrelation. The applied regularization procedure revealed that the data acquired with the novel methodology indeed resulted in a data set free of visible spatial aliasing.

ACKNOWLEDGMENTS

The authors acknowledge Deltares and the Royal Netherlands Institute for Sea Research for their essential contribution to the field experiment. We sincerely thank Gábor Bada from the ELTE University in Hungary, Wim Versteeg from Ghent University in Belgium, and the students Koen Duijnmayer from Delft University of Technology and Atilla Deák and Istvan Kuda from the ELTE University. We are also grateful to Alber Hemstede for his technical support. Finally, we acknowledge the reviewers for their valuable comments. This work is sponsored by the Netherlands Research Centre for Integrated Solid Earth Sciences (ISES).

REFERENCES

Ayres, A., and F. Theilen, 1999, Relationship between P- and S-wave velocities and geological properties of near-surface sediments of the continental slope of the Barents Sea: Geophysical Prospecting, **47**, no. 4, 431–441.

Chapman, N. R., J. F. Gettrust, R. Walia, D. Hannay, G. D. Spence, W. T. Wood, and R. D. Hyndman, 2002, High-resolution, deep-towed, multichannel seismic survey of deep-sea gas hydrates off western Canada: Geophysics, **67**, 1038–1047.

Duijndam, A. J. W., M. A. Schonewille, and C. O. H. Hindriks, 1999, Reconstruction of band-limited signals, irregularly sampled along one spatial direction: Geophysics, **64**, 524–538.

Hale, D., 2009, A method for estimating apparent displacement vectors from time-lapse seismic images: Geophysics, **74**, no. 5, V99–V107.

Hamilton, E. L., 1979, V_p/V_s and Poisson's ratios in marine sediments and rocks: Journal of the Acoustical Society of America, **66**, 1093–1101.

He, T., G. D. Spence, W. T. Wood, M. Riedel, and R. D. Hyndman, 2009, Imaging a hydrate-related cold vent offshore Vancouver Island from deep-towed multichannel seismic data: Geophysics, **74**, no. 2, B23–B36.

Kabir, M. M. N., and D. J. Verschuur, 1995, Restoration of missing offsets by parabolic Radon transform: Geophysical Prospecting, **43**, no. 3, 347–368.

Lucas, A. L., 1974, A high resolution marine seismic survey: Geophysical Prospecting, **22**, no. 4, 667–682.

Marsset, B., T. Missiaen, Y. H. De Roeck, M. Noble, W. Versteeg, and J. P. Henriet, 1998, Very high resolution 3D marine seismic data processing for geotechnical applications: Geophysical Prospecting, **46**, no. 2, 105–120.

Müller, C., B. Milkereit, T. Bohlen, and F. Theilen, 2002, Towards high-resolution 3D marine seismic surveying using Boomer sources: Geophysical Prospecting, **50**, no. 5, 517–526.

Pinson, L. J. W., T. J. Henstock, J. K. Dix, and J. M. Bull, 2008, Estimating quality factor and mean grain size of sediments from high-resolution marine seismic data: Geophysics, **73**, no. 4, G19–G28.

Pulliam, J., J. A. Austin, E. C. Luhurbudi, S. Saustrup, and P. L. Stoffa, 1996, An ultrahigh resolution 3-D survey of the shallow subsurface on the continental shelf of New Jersey: The Leading Edge, **15**, no. 7, 839–845.

Schuster, G. T., and M. Zhou, 2006, A theoretical overview of model-based and correlation-based redatuming methods: Geophysics, **71**, no. 4, SI103–SI110.

Stewart, R. R., J. E. Gaiser, R. J. Brown, and D. C. Lawton, 2003, Converted-wave seismic exploration: Applications: Geophysics, **68**, 40–57.

Taner, M. T., F. Koehler, and K. A. Alhilali, 1974, Estimation and correction of near-surface time anomalies: Geophysics, **39**, 441–463.